Predictions of the Initial Non-Steady-State Crack Growth Behavior in the Creep/Fatigue of the Nickel-Base Superalloy AP1

K.M. Nikbin

Using the fracture mechanics parameters K and C^* to analyze cyclic crack growth test results carried out on the nickel-base superalloy AP1, the effects of test frequency on the initial incubation time followed by transient cracking rates and the steady-state secondary crack growth rates were considered. The cracking behavior at 700 °C for this material exhibits a frequency dependence over a range of 0.001 to 10 Hz. It has been shown that, at high temperatures under steady-state cracking conditions, fatigue processes are most dominant at high frequencies, and conversely, time-dependent creep dominates at low frequencies. The creep cracking rate is described by a model linked to the exhaustion of available ductility in a creep process zone at the crack tip, and the fatigue rate is linked to the Paris Law equation. For the secondary regime of crack growth, the effects of frequency are described in a cumulative damage model developed for creep/fatigue interaction. For the crack incubation and the transient process under initial loading, the model is extended to predict the cracking behavior in the creep regime at low cyclic frequencies. For the higher frequencies, fatigue dominates and creep transient effects are not observed experimentally.

Keywords

crack growth modeling, creep/fatigue crack growth, cumulative damage, incubation, nickel-base superalloy, steady-state cracking, transient crack growth

1. Introduction

MANY nickel-base superalloy components in gas turbines, power plants, and nuclear reactors undergo cyclic loading during their operating life at high temperatures, and their permitted design tolerances against creep deformation need to be restricted due to operational and safety considerations. The mechanical and geometric constraints used in the design of these components, regardless of their creep ductility, invariably produce creep-brittle crack growth and failures in which creep damage is localized. Therefore, under plane-strain conditions, it is possible to induce a crack in a material with a high uniaxial creep ductility and fatigue toughness if the crack tip damage is contained locally by means of a geometric constraint or some form of material degradation and/or testing variable. The creep/fatigue and environmental processes will thus contribute to crack tip-controlled failures in these alloys. The dominant mode of fracture will therefore depend on such factors as material composition, heat treatment, cyclic to mean ratio, frequency and temperature, and operating environment.[1-3]

The applicability of linear and nonlinear fracture mechanics crack growth models based on K and C^* depending on the state of stress of the particular test condition at the crack tip has become accepted[2-6] for the secondary steady-state stage of cracking. The initial incubation and transient stages of cracking still require further analysis. Models developed for this initial behavior are applied to tests carried out on a nickel-base superalloy (AP1)[2] (see Table 1) under cyclic loading over a range of frequencies between 0.001 to 10 Hz. In this article, the transition from an elastic to a creep steady state of stress is modeled to describe the initial cyclic crack growth behavior. The characterization of cracking rates in the early stage of incubation and damage accumulation on first loading is described in terms of initial incubation time followed by the gradual increase in crack growth to coincide with the steady-state cracking rate. Using the experimental data from AP1, damage due to creep and fatigue are described in terms of a cumulative damage model and then linked to a model to describe the transition phenomenon to bound the crack growth behavior in the initial and the secondary stage of cracking.

K.M. Nikbin, Department of Mechanical Engineering, Imperial College, London SW7 2BX.

2. Experimental Procedure

Details of the materials and experimental procedure have been presented previously,[2] and only an outline will be included here. The nickel-base superalloy that was examined is designated AP1. It was received in the form of a hot isostatically pressed billet that was heat treated to produce a microstructure containing approximately 40 vol% of γ' phase dispersed in a γ-nickel solid solution matrix with an average grain size of 60 μm. The material was tested at 700 °C, R ratio of 0.7, frequency range of 0, and 0.001 to 10 Hz in the form of standard and initially prefatigued compact tension specimens 50 mm wide and 25 and 12 mm thick containing no side grooves.

2.1 *Modeling Cyclic Crack Growth Behavior*

The creep/fatigue crack growth analysis for this material must contain two modes of behavior. These are time-inde-

pendent fatigue and time-dependent creep cracking modes. The fact that in the time-dependent regime the cracking rate is not necessarily steady state[3,7] adds an additional variable that must be taken into account. A model that considers all of the aspects of cracking behavior is thus needed for use in life prediction methods and the section below describes such a model and its application to the AP1 nickel-base superalloy.

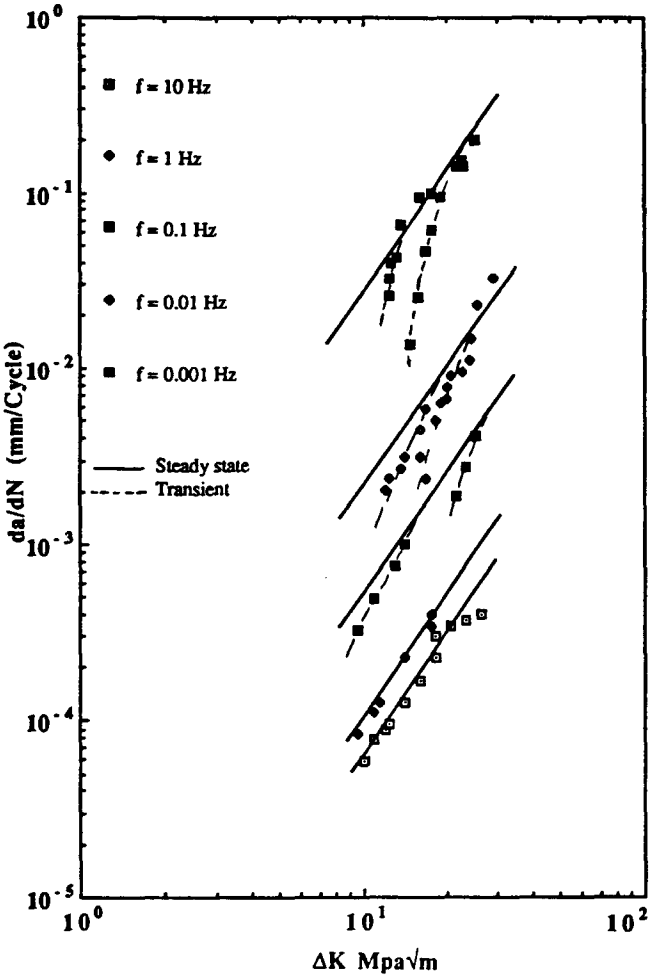

Fig. 1 Example of transient effects in the correlation of crack growth versus ΔK for AP1; CT specimens tested at 700 °C at various frequencies and $R = 0.7$.

2.2 *Fatigue Analysis*

When a cracked test piece is cyclically loaded at room temperature in the absence of any environmental conditions, the cracking rate is cycle dependent and fatigue processes dominate. A fatigue threshold exists below which no crack growth can be obtained but the secondary steady-state crack growth per cycle is time dependent and is given in terms of *da/dN* such that

$$\frac{da}{dN} \alpha \Delta K^m \quad [1]$$

where *da/dN* is the crack growth per cycle; *K* is the stress-intensity factor; and *m* is a material constant that has a typical value of 2 to 4 for most engineering materials. At higher temperatures where cyclic loading is used, Eq 1 generally describes the secondary cracking behavior of the material. Previous work on high-temperature cyclic crack growth[2,3] has shown that a change in frequency affects the creep/fatigue interaction and transition points.

When the load is cycled or when temperature transients produce cyclic loading on the structure, both time-independent fatigue and time-dependent cracking behavior can be observed. Generally, when creep and time-dependent mechanisms are involved, fracture is intergranular, and when cycle-dependent fatigue processes dominate, failure is transgranular.[2] In the range of creep-dominant cracking behavior, at low cyclic rates, it is more appropriate[3-7] to use nonlinear fracture mechanics concepts and express the steady-state time-dependent cracking rate $\dot{a}$ as a function of the creep fracture mechanics parameter C^* by assuming that the creep strain rate $\dot{\varepsilon}$ is governed by the Norton's creep rate:[5,6]

$$\dot{\varepsilon} = C\sigma^n \quad [2]$$

which yields for a cracked body[5]

$$\dot{a} = D_o C^* \varphi \quad [3]$$

or

$$da/dN = (D_o C^* \varphi)/f \quad [4]$$

Table 1 Composition, heat treatment, and creep properties of alloy AP1
Heat treatment: 4 h 1100 °C, AC, 24 h 650 °C, AC, 8 h 760 °C, AC

Composition, wt%							
Cr	Mo	Ti	Al	Zr	C	B	Ni
14.8	5.04	3.5	3.98	0.04	0.02	0.0002	bal

Creep properties at 700 °C					
Material	*n*	σ_o	*D*	φ	ε_f
AP1	8	1100	5	0.88	0.15

Note: σ_o (MPa) at $\dot{\varepsilon}_o = 1/h$; *n*, the creep index, and ε_f, the uniaxial ductility (as a fraction), have been evaluated from rupture data; $D = D_o/\varepsilon^* f$ is the constant in Eq 3 when C^* is in MJ/m^2·h and $\varphi = n/n + 1$). AC, air cooled; geometry, compact tension.

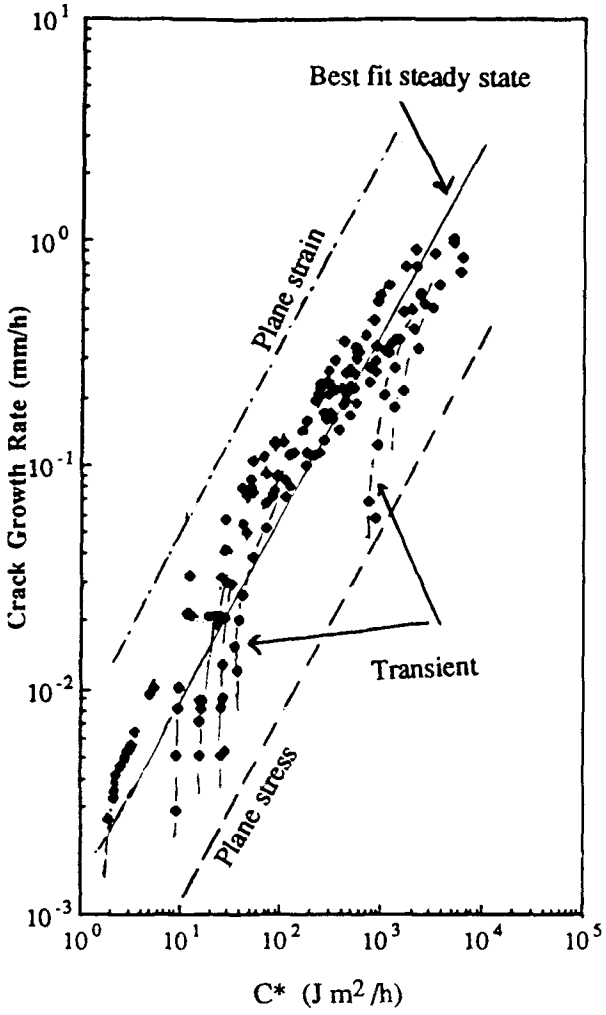

Fig. 2 Example of transient effects in the correlation of crack growth versus C^* for AP1; CT specimens tested at 700 °C.

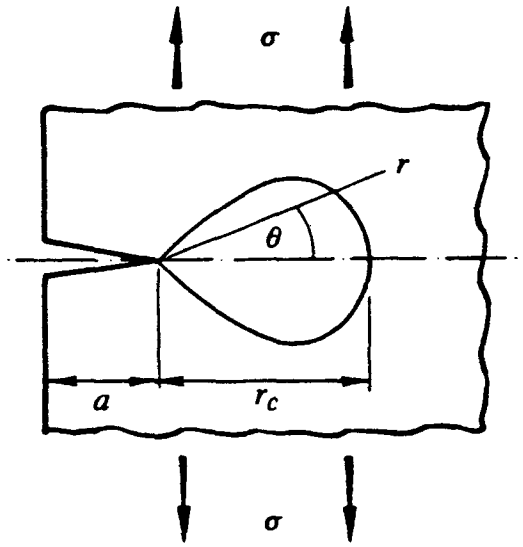

Fig. 3(a) Model of a creep process zone ahead of a crack tip.

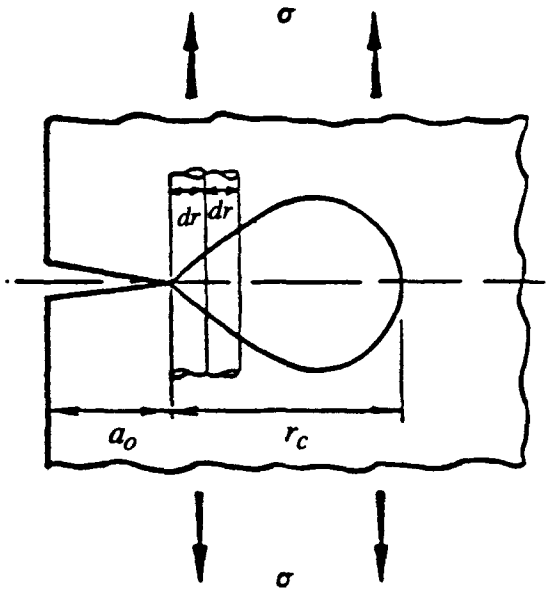

Fig. 3(b) Ligament damage development in a creep process zone.

where $\varphi = (n/n + 1)$, a number slightly less than unity, and C are material constants; n is the creep index in Norton's creep law; f is the frequency; N is the number of cycles; C^* is the nonlinear creep parameter evaluated at maximum load; and D_o is the proportionality factor determined primarily by the material creep ductility and the constraint local to the crack tip. An increase in crack growth is obtained by an increase in the degree of constraint and with a decrease in ductility. Therefore, material cracking behavior will be controlled by both the material creep properties, specimen geometry, and test variables such as temperature and frequency. Equation 3 has been shown to describe time-dependent cracking behavior over a range of crack tip constraints,[7] and a general model to describe creep crack growth from plane stress to plane strain is given as:

$$\dot{a} = 3C^*\varphi/\varepsilon^*_f \qquad [5]$$

where $\dot{a}$ is in mm/h; C^* in MJ/m^2·h; and the creep strain, ε_f^*, is a fraction; ε_f^* is taken as the material uniaxial creep ductility ε_f in plane stress and as $\varepsilon_f/50$ for the case of plane-strain.[8] Generally, in the low-cyclic frequency range before creep redistribution occurs, K describes the crack tip linear stresses, but with the advance of damage with time, C^* will be applicable. However, in the initial stages of loading and damage accumulation, K and the steady-state model of C^* fails to adequately describe the process of crack initiation and growth. Figures 1 and 2 show representative examples of the "tail" that exists in crack growth versus K and C^* data for the nickel-base superalloy AP1 tested at various frequencies at 700 °C. The initial transi-

tion tail constitutes a substantial part of test times, and the modeling of this feature would improve cyclic crack growth rate predictions using the C^* parameter.

To predict crack growth at high temperatures, a process zone (Fig. 3a) can be postulated at the crack tip[9] where cracking proceeds when an element of material experiences damage and rupture stressed according to the local magnified state of stress. This nonlinear stress singularity determines the rate at which the element of material accumulates damage, and failure occurs when the creep ductility, ε_f^*, appropriate to the state of stress (or to the extent of constraint) at the crack tip is exhausted. For the case of plane stress ($\varepsilon_f^* = \varepsilon_f$, where ε_f is the uniaxial creep ductility) the Nikbin, Smith, and Webster model[9] of steady-state creep crack growth yields $\dot{a}_s$ in the form:

$$\dot{a}_s = \left\{(n+1)/\varepsilon_f^*\right\}\left[C^*/I_n\right]^{n/(n+1)}(Ar_c)^{1/(n+1)} \quad [6]$$

where I_n is a nondimensional function of n; r_c is the creep process zone size over which each element experiences the appropriate stress history; and A is a material constant. This expression assumes the development of steady-state damage distribution in the region of the process zone. It assumes that zero damage exists at $r = r_c$ and that progressively more damage is accumulated as the crack tip is approached. Therefore, the model assumes that some additional strain is required to break a ligament dr at the crack tip because it will be almost broken before the crack reaches it.

2.3 *Transient Analysis*

As previously stated, the experimental evidence from AP1, both in terms of K and C^*, as shown in Fig. 1 and 2, suggests that the initial loading produces a tail in the crack growth, which can be attributed to time-dependent creep transition behavior. This phenomenon has also been described mathematically in Ref 10 and 11. This transition effect would be mainly attributed to the transition time, which is described as the time required to go from an elastic state of stress at the crack tip to a steady-state creep stress.[7,12] By eliminating the data points up to the point of the transition time, the actual periods of the tail that have been measured experimentally are still apparent in the test data, suggesting that on first loading the steady-state conditions at the crack tip will not exist. At first loading, a stable distribution of damage will need to build up ahead of the crack before steady-state crack growth begins. The small ligament dr (Fig. 3b) will not have suffered any creep strain, and failure will not occur until a time dt has elapsed, given by:

$$\varepsilon_f^* = \dot{\varepsilon}dt \quad [7]$$

where $\dot{\varepsilon}$ is the creep displacement rate. This leads to an initial creep crack growth rate, $\dot{a}_o$, yielding

$$\dot{a}_o = dr/dt \quad [8]$$

yielding

$$\dot{a}_o = (1/\varepsilon_f^*)\left[C^*/I_n\right]^{n/(n+1)}(A_{dr})^{1/(n+1)} \quad [9]$$

Equation 9 is very similar to that derived from the steady-state damage conditions (Eq 6). It results in the relation

$$\dot{a}_o = (1/n+1)\,(dr/r_c)^{1/(n+1)}\dot{a}_s \quad [10]$$

the ligament dr can be chosen to be a suitable fraction of r_c. However, because dr/r_c is raised to a small power in Eq 10:

$$\dot{a}_o \approx (1/n+1)\dot{a}_s \quad [11]$$

For most engineering materials, therefore, the initial crack growth rate is expected to be approximately an order of magnitude less than that predicted from the steady-state analysis. The cracking rate will progressively reach the steady-state cracking rate as damage is accumulated. Numerical integration is required to evaluate Eq 10. A computer program has been developed, using incremental crack extension, to evaluate the transition period resulting from the development and the accumulation of damage in accordance with Eq 6 and 10.

2.4 *Prediction of Incubation Periods*

Various models incorporating crack opening displacement information from tests have been developed.[13-15] These types of data have not always been recorded, and moreover, they are more appropriate for use in creep ductile materials. Therefore, given that in most high-temperature tests there is an incubation period that is attributable to the time required for the crack to initiate to a physically measurable (only limited by the crack measuring techniques used) size, the present models of creep crack growth can then be developed to calculate an incubation period using crack length as a basis for crack initiation. The model gives equations for cracking rate that are not sensitive to the process zone size, because r_c is raised to a small fractional power in the model. However, from microstructural observations,[2] r_c usually can be taken to be about the material grain size. This size also corresponds reasonably with the limit of detection of most crack monitoring systems (50 to 100 μm). Consequently, in this analysis, it will be assumed that crack initiation takes place when the crack has extended a distance r_c so that the incubation period t_i becomes

$$t_i = \int_o^{r_c}\frac{dr}{\dot{a}} \quad [12]$$

where $\dot{a}$ will increase from its initial transient value $\dot{a}_o$ to $\dot{a}_s$ with crack extension. A lower bound estimate of t_i can be obtained by substituting $\dot{a} = \dot{a}_s$ using Eq 1, 4, and 5 to yield:

$$t_i = r_c/\dot{a}_s = \left(r_c^{n/(n+1)}\varepsilon_f^*\right)/\left((n+1)[C^*/I_n]^{n/(n+1)}A^{1/(n+1)}\right) \quad [13]$$

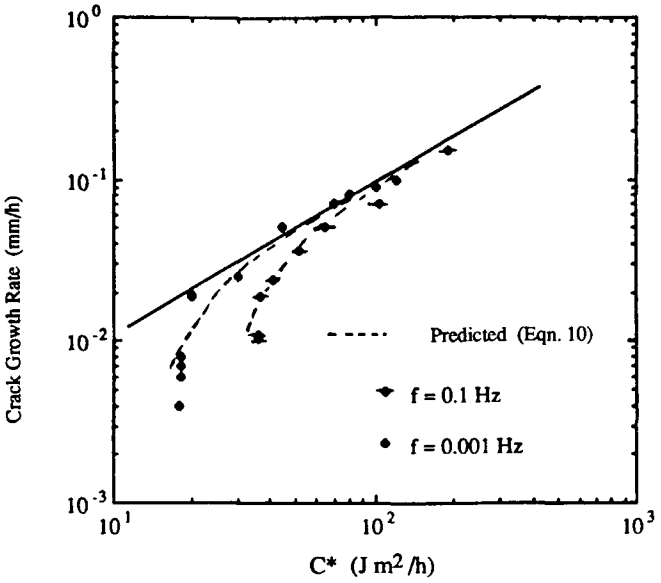

Fig. 4 Sample prediction of the primary and secondary cracking rates using Eq 10.

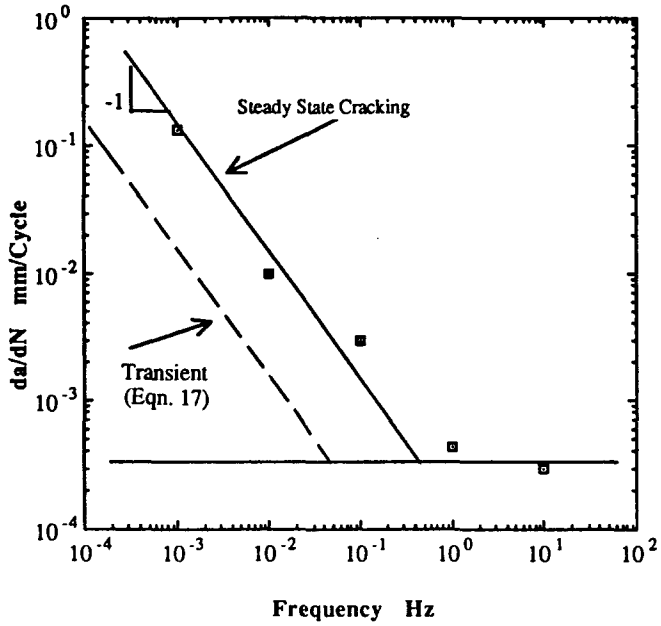

Fig. 5 Frequency dependence of da / dN at ΔK = 20 MPa$\sqrt{m}$ for API at 700 °C.

Some indication of an upper bound can be determined by taking $\dot{a}$ to equal $\dot{a}_o$ from Eq 9 so that

$$t_i = r_c \varepsilon_f^* / \left([C^*/I_n]^{n/(n+1)} (A_{dr})^{1/(n+1)} \right) \quad [14]$$

Equations 13 and 14 can, therefore, be used to provide estimates of incubation periods for crack growth from a knowledge only of uniaxial creep and stress-rupture data. An estimate of the incubation period can also be obtained by using the approximate steady-state creep crack growth law (Eq 5). If this is used for steady-state conditions, a lower bound to the incubation period in hours becomes

$$t_i \approx r_c \varepsilon_f^* / 3C^{*0.85} \quad [15]$$

with ε_f^* as a fraction and C^* in MJ/m^2·h. The approximate crack growth law assumes n = 5.7, to yield φ = 0.85. Consequently, from Eq 11, if the incubation period is calculated from the initial transient cracking rate $\dot{a}_o$ determined from Eq 6:

$$t_i \approx (n+1) r_c \varepsilon_f^* / 3C^{*0.85} \quad [16]$$

Equations 13 to 16 can then be applied to experimental data taken from creep crack growth tests. An example of the application of this model to API tested at 700 °C is used in the next section to relate experimental initiation times for the compact specimens tested at frequencies of less than 0.1 Hz to the predictions approximated in Eq 15 and 16.

3. Results

Figure 1 shows the cyclic crack growth data for the entire frequency range of 0.001 to 10 Hz plotted versus ΔK, and Fig. 2 shows the low-cycle crack growth data for the frequency range of 0.1 to 0.001 Hz plotted versus C^*. Figure 1 shows that the effect of transient cracking increases with a reduction in the frequency, suggesting that this is a time-dependent phenomena. Figure 2 shows that the effect is independent of the C^* value and only occurs on initial loading. The upper and lower bound predictions for the plane-strain and plane-stress cracking rates evaluated from Eq 5 are also shown in Fig. 2. The best average line drawn through the data provides an effective creep ductility at the crack tip ε_f^* = 0.018 for the present API data.

A comparison of the experimental cracking rate and the predicted rate is shown in Fig. 4. The predicted results show that the trends at the initial stages of the cracking rates, where a tail exists in the experimental data, are predicted satisfactorily by the model. The values of D_o and φ used in Eq 3 determine the accuracy with which the steady-state crack growth rates are predicted. There are no visible differences. All show varying degrees of an initial tail, and the model describes the transition to steady state within a factor of two or less.

4. Discussion and Conclusions

It has been observed that this transition period to steady-state C^* is not sufficient to explain the tail that exists in the low-cycle creep crack growth data. Expressions developed to predict initial ligament damage accumulation at the crack tip have been applied to a nickel-base superalloy.

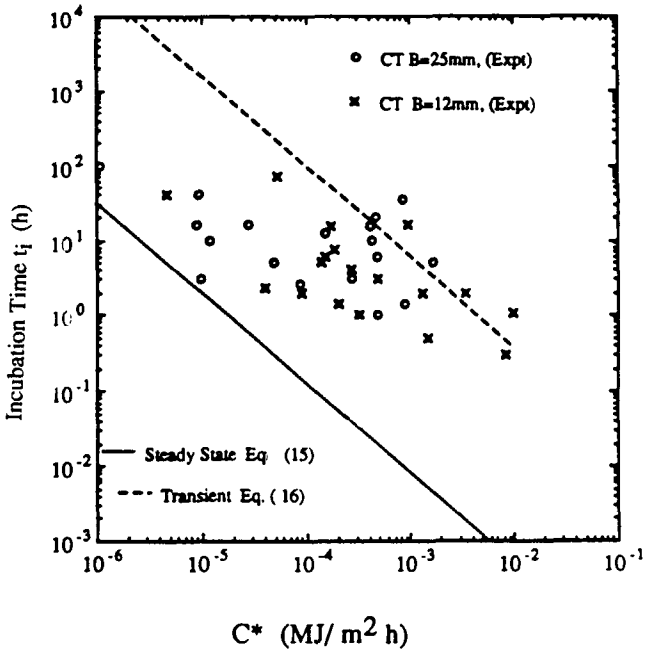

Fig. 6 Experimental and predicted incubation times versus C^* for AP1 at 700 °C.

The predicted results show that the initial cracking rate $\dot{a}_o$ could be up to approximately one tenth of the steady-state crack growth rate $\dot{a}_s$. This value is consistent with the experimental data for the four alloys considered. The period over which the transition takes place in the predictions has also been found to be up to 40% of the total life, and it compares well with the first stage crack initiation and growth times found experimentally. Because the ideal secondary steady state does not exist in the laboratory data and primary and tertiary effects are prevalent to varying degrees, the present predictions, using the ligament damage development model, show the correct trends but would be dependent on the accuracy of the C^* estimation procedure used.

To predict cyclic low-frequency crack growth at high temperatures, the small ligaments ahead of the crack in the process zone are assumed to behave time independently and will not have suffered any creep strain initially, and failure will not occur until time has elapsed to accumulate sufficient creep strains for an increment of crack to advance. This leads to an initial crack growth rate $\dot{a}_o$ given approximately as

$$\dot{a}_o \approx (1/n+1)\dot{a}_s \qquad [17]$$

where $\dot{a}_s$ is the steady-state cracking rate. For most engineering materials under cyclic loading, therefore, the initial crack growth rate is expected to be approximately an order of magnitude less than that predicted from the steady-state analysis. The cracking rate will progressively reach the steady-state cracking rate as damage is accumulated.

For cyclic loading, a damage accumulation model[2] gives

$$da/dN = (da/dN)_t + (da/dN)_f \qquad [18]$$

where t and f refer to the time- and cycle-dependent mode of cracking. Assuming time-dependent cracking only occurs at maximum load in the cyclic tests

$$da/dN = \dot{a}/3600f + C'\Delta K^m \qquad [19]$$

where da/dN is in mm/cycle; $\dot{a}$ in mm/h; and C' is a material constant. This model suggests that creep and fatigue are accumulative. The frequency range of the creep fatigue interaction can thus be determined, and because fatigue is time independent only the creep time-dependent processes will vary the interaction range. Figure 5 shows the frequency cumulative damage model as given in Eq 19. The secondary cracking rate values are plotted at a constant value of $\Delta K = 20\text{MPa}\sqrt{\text{m}}$ versus frequency. The dashed line uses Eq 17 to predict the lower bound for the creep/fatigue interaction for AP1. Because the fatigue process is independent of time, all transient effects would be due to creep and the nonlinear state of stress at the crack tip. The effect of the transient on the creep/fatigue range is that fatigue will be dominant at a frequency below 0.01 Hz, suggesting that the loading and unloading cycles could prolong the transient behavior and the accumulation of sufficient creep damage for the secondary state of cyclic crack growth.

The predictions for the incubation periods are shown in Fig. 6 The value of r_c used is the grain size (Table 1), and Eq 15 and 16 were used to predict the upper and lower bounds of the prediction lines. Because AP1 material is a fairly creep-brittle material that shows no creep deformation of the geometry, it has a small ratio of incubation time in relation to the total life. Hence, for the lower, experimental C^* values, a shallower slope is evident in the figure, suggesting relatively smaller incubation periods compared to the lower bound predicted lines taken from Eq 15. For the higher C^* values, the incubation times are greater relative to the lower bound predictions. Slowing of the crack growth initiation may be attributed to the crack tip plasticity that occurs when a large load is applied. From Fig. 6, it is clear that, for a safe prediction of the initiation times for the present test conditions, the lower bound line is given by

$$t_i \approx r_c \varepsilon_f^* / 3C^{*0.85} \qquad [20]$$

where ε_f^* is the taken as the uniaxial creep ductility, $\varepsilon_f/8$ from the best fit line of data in Fig. 2. Also from Eq 12, it is clear that the rate of damage buildup will determine the incubation time, and this is dependent on the chosen value of r_c. The faster the buildup of damage, the closer the steady-state prediction lines to data points, as in Fig. 6, and when it develops slowly, the agreement is nearer the transient prediction line. The present laboratory tests are relatively short, and results from longer term tests that are more in line with component life times should be used to provide further support for this model.

In considering the test data for AP1, it has been shown that the model of the creep process zone at the crack tip can be used to describe the incubation, transient, and steady-state crack growth behavior of this material. Approximate terms of the

model, requiring basic available uniaxial and crack growth data, have been put forward for use as life prediction criteria of other engineering materials.

Acknowledgments

The author would like to thank the Defence Research Agency (Pyestock) for their financial backing of this project.

References

1. A. Pineau, *Fatigue at High Temperature*, R.P. Skelton, Ed., Applied Science, London, 1983
2. M.R. Winstone, K.M. Nikbin, and G.A. Webster, Models of Failure under Creep/Fatigue Loading of a Nickel-Based Superalloy, *J. Mater. Sci.*, Vol 20, 1985, p 2471-2476
3. V. Dimopulos, K.M. Nikbin, and G.A. Webster, "Influence of Cyclic to Mean Load Ratio on Creep/Fatigue Crack Growth," ASM Materials Week '86, 1986
4. K.M. Nikbin, K. Nishida, and G.A. Webster, "Creep/Fatigue Crack Growth in a 10% Cr Martensitic Steel," ICM6, Japan, Aug 1991, *Metall. Trans.*, 19A, 1986, 873-880
5. K.M. Nikbin, D.J. Smith, and G.A. Webster, An Engineering Approach to the Prediction of Creep Crack Growth, *J. Eng. Mater. Technol.*, Vol 108, 1986, p 186-191
6. R.A. Ainsworth and I.W. Goodall, Defect Assessment at Elevated Temperatures, *J. Pressure Vessel Technol.*, Vol 105, 1983, p 263-268
7. K.M. Nikbin, Transition Effects in Creep-Brittle Materials, in *Mechanics of Creep Brittle Materials*, Vol 2, A.C.F. Cocks and A.R.S. Ponter, Ed., Elsevier Applied Science, 1991, p 14-24
8. G.A Webster, Crack Growth at High Temperature, in *Engineering Approaches to High Temperature Design*, B. Wilshire and D.R.J. Owen, Ed., Pineridge Press, Swansea, 1983, p 1-56
9. K.M. Nikbin, D.J. Smith, and G.A. Webster, Influence of Creep Ductility and State of Stress on Creep Crack Growth, in *Advances in Life Prediction Methods at Elevated Temperatures*, D.A. Woodford and J.R. Whitehead, Ed., ASME, 1983, p 249-258
10. S. Kubo, K. Ohji, and K. Ogura, An Analysis of Creep Crack Propagation on the Basis of the Plastic Singular Stress Field, *Eng. Fract. Mech.*, Vol 11, 1979, p 315-329
11. H. Riedel, The Extension of a Macroscopic Crack at Elevated Temperature by the Growth and Coalescence of Microvoids, in *Creep in Structures*, A.R.S. Ponter and D.R. Hayhurst, Ed., Springer-Verlag, Berlin, 1981, p 514-519
12. H. Riedel and J.R. Rice, Tensile Cracks in Creeping Solids, in *Fracture Mechanics*, ASTM STP 700, 1980, p 112-130
13. R.A. Ainsworth, The Initiation of Creep Crack Growth, *Int. J. Solids Struct.*, Vol 18, 1982, p 873-881
14. G.J. Neate, Creep Crack Growth in ½ CrMoV Steel at 838 K. I: Behavior at a Constant Load, *Mater. Sci. Eng.*, Vol 82, 1986, p 59-76
15. R. Piques, Ph. Bensussan, and A. Pineau, Crack Initiation and Growth under Creep and Fatigue Loading of an Austenitic Stainless Steel, *Nucl. Eng. Design*, Vol 116, 1989, p 293-306